

SHEAR STRENGTH OF ASR-DETERIORATED RC MEMBERS AND SHEAR REINFORCING EFFECT OF REPAIR BY ADDING REBAR

KOICHI KOBAYASHI*, TAKAHIRO FUKUSHIMA[†] AND KEITETSU ROKUGO[†]

* Gifu University
Yanagido 1-1, 511193, Gifu, Japan
e-mail: ko2ba@gifu-u.ac.jp

[†]Gifu University

Key words: ASR, Shear strength, Rebar adding repair, Shear strengthening

Abstract: This study aims at clarifying the effects of rebar rapture caused by ASR on the mechanical performance of RC members. Rapture of tensile or shear reinforcement was simulated in RC beam specimens, which were subjected to a bending test after deteriorated by ASR. Some of the beams were repaired by adding rebars, and the effects of the repair were investigated. The results showed that the ASR increased the shear strength of the beams with less shear reinforcement, and caused a reduction in bond between the tensile rebar and cover concrete. It was also found out that the repair by adding rebar may not necessarily be effective when the integrity of the concrete has been lost due to cracks propagating by the ASR.

1 INTRODUCTION

In Japan, rapture at the bend of reinforcement in RC structures caused by ASR has been frequently reported in the last decade [1]. Rebar suffering rapture at the bend may lose its bond and anchorage and may be pulled out, which will deteriorate mechanical performances of RC the structure [2-3]. However, the mechanical properties of RC structures suffering ASR and raptured rebar are yet to be clarified.

In this study, RC beam specimens were prepared using a reactive aggregate and kept in a humid room to accelerate ASR deterioration. A bending test was conducted after that to investigate the effects of the difference in the amount and anchorage condition of the tensile and shear reinforcement on the mechanical performance of the ASR-deteriorated RC members. Some of the deteriorated beams were repaired by adding rebar, and the effects of the shear strengthening were investigated.

2 EXPERIMENTAL PROCEDURE

2.1 Materials and mixtures

Table 1 shows three concrete mixtures used in this study: A normal concrete mixture without reactive aggregate (NC), a mixture using both fine and coarse reactive aggregates (SG), and a mixture using a coarse reactive aggregate (G). Ordinary Portland cement was employed for all the mixtures, and the water-cement ratio was 0.57. The reactive aggregates were crushed sand and crushed stone of andesite. Mixing ratios of reactive and non-reactive aggregates were 70:30 for the fine aggregate and 50:50 for the coarse aggregate. These ratios were set based on the pessimum values that were determined through a preliminary test. Sodium chloride was added to the ASR mixtures so that the equivalent amount of alkali was 12kg/m³. Non-shrink mortar with a water-cement ratio of 0.46 was used for grouting in repair for the shear strengthening by adding rebar.

Table 1: Mixtures of concrete

	W/C	s/a	Unit mass kg/m ³	Ratio of Reactive aggregate		
				W	S	
			NC	0.57	0.474	
SG	168	0.7	0.5			*2
G		0				

*1: 0.79kg/m³ of WRA

*2: 19.5kg of sodium chloride (NaCl)

2.2 Specimens

Table 2 shows a list of the specimens. Figures 1 and 2 are the schematics of the beam specimens. 3-D13 steel bars with a nominal yield strength of 345N/mm² were used for the tensile reinforcement. Lateral confinement of D6 steel bars were arranged at an equal interval of 100 mm within a pure bending span in all the beam specimens to allow for later comparison of failure mode in the shear span. In addition to RC beams with tensile reinforcement having hooks at both ends, beams without hooks were prepared in order to simulate a rapture at the anchorage of tensile reinforcement by ASR expansion. In addition to the specimens with shear-reinforcing D6 stirrups spaced at 100mm intervals within shear spans (hereafter referred to as “Series D6”), specimens with φ3 stirrups spaced at 100mm intervals (as “Series φ3”) and specimens without stirrups (as “Series 0”) were prepared to simulate decreasing of shear reinforcement due to the rapture of the stirrups. Two beams each were prepared for each type of the specimens. The specimens with reactive aggregate were kept in a chamber in which the temperature was kept between 35 and 40 degrees Celsius, with the relative humidity kept around 100% to accelerate deterioration.

Table 2: List of specimens

	Stirrup	Hooks for tensile rebar	Mixture
Series D6	D6	Yes	NC / SG / G
		No	
Series φ3	φ3	Yes	
		No	
Series 0	none	Yes	
		No	

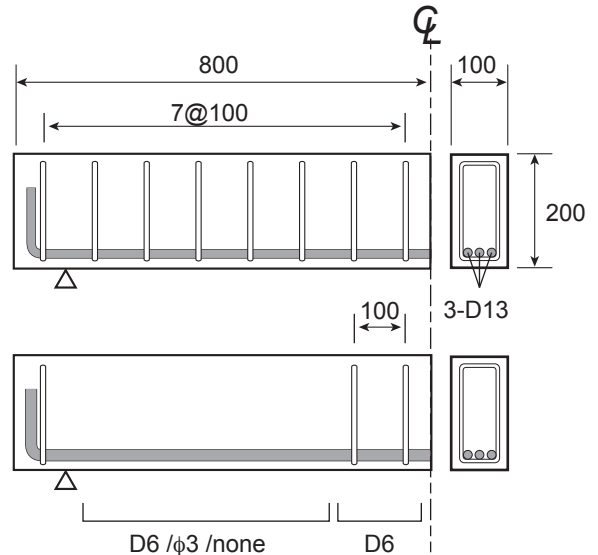


Figure 1: Loading test beams with hooks (unit: mm)

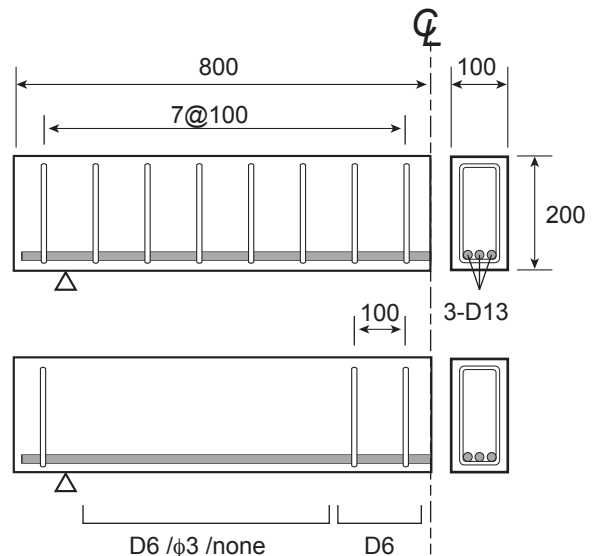


Figure 2: Loading test beams without hook (unit: mm)

2.3 Length change measurement

As shown in Figure 3 eight plugs were embedded in each beam for measuring a length change of the concrete by a contact gauge method. The gauge length was 100mm

along the vertical direction, and 200mm along the longitudinal direction of the specimen.

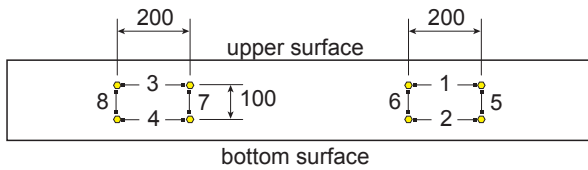


Figure 3: Plug arrangement for expansion measurement (unit: mm)

2.4 Shear strengthening

Shear strengthening [4] was applied to two beams of Series $\phi 3$ with mixture G, one with tensile rebar hooks and one without, and two beams of Series 0 with mixture G, one with tensile rebar hooks and one without, i.e., a total of four specimens. Twelve holes with a diameter of 22mm and a depth of 160mm, which equals to the distance between the concrete upper surface and the tensile reinforcing rebar, were drilled to the ASR-deteriorated specimens with a spacing of 100mm using a core drill. Two each 160mm long D6 bars were inserted into the respective holes, which were then filled with non-shrink mortar. Figures 4 and 5 show the schematics of the thus repaired Series $\phi 3$ specimens and Series 0 specimens, respectively.

2.5 Bending test

A two-point loading test was performed to the beams of mixture NC at the age of 28days, and to the beams of mixtures SG and G after being left in a high-humidity, high temperature chamber for one year for deterioration, with a constant moment span of 300mm, a shear span of 550mm, and a shear span ratio of $a/d=3.10$, as shown in Figure 6. Displacements were measured with high-sensitivity displacement transducers at the two supporting points, two loading points, and the mid point. Eight Pi gauges were set to measure the width of bending cracks, shear cracks, and bond splitting cracks caused by the pull-out of the tensile rebar.

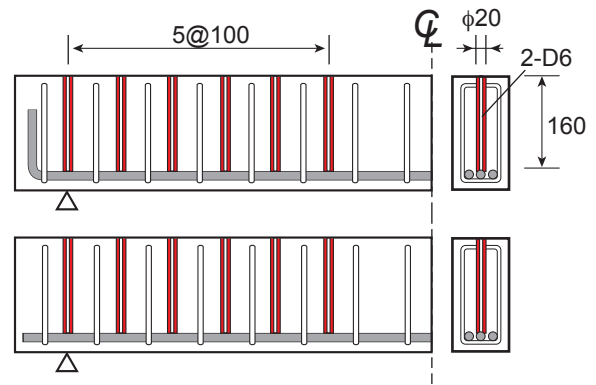


Figure 4: Shear strengthening for Series $\phi 3$ specimens (unit: mm)

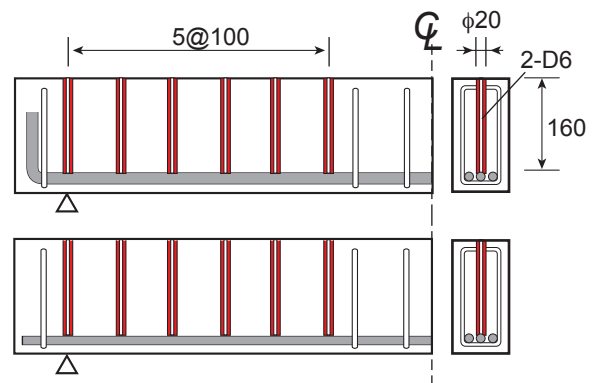


Figure 5: Shear strengthening for Series 0 specimens (unit: mm)

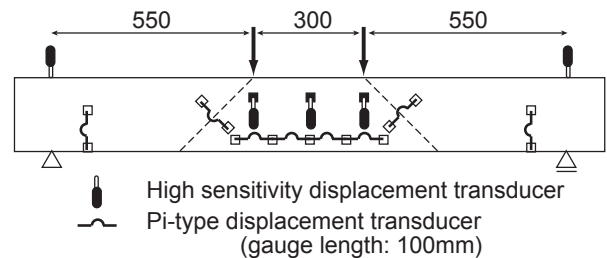


Figure 6: Setup for loading test (unit: mm)

3 DETERIORATION BY ASR

3.1 Compressive strength

Table 3 shows the compressive strength of mixtures NC, SG, and G. Note that the compressive strength and the elastic modulus of mixtures SG and G were measured both before the ASR deterioration (28days age) and after the deterioration (1year age). Cracks were visible on the surface of the ASR-deteriorated SG and G concrete. While both SG and G concrete had a lower elastic modulus after the deterioration, the decrease

being more remarkable with SG concrete, the compressive strength of SG concrete slightly increased. This increase is considered to be due to the progress of cement hydration during the ASR deterioration acceleration period of one year. Namely, it is assumed that the specimens at early ages did not exhibit their full strength as Sodium ions inhibited the hydration, which then progressed during the one year.

Table 3: Compressive strength of concrete

Mixture	Test age	Comp. strength N/mm ²	Young's modulus KN/mm ²
NC	28days	41.7	31.5
SG	28days	28.5	26.0
	About 1year	33.3	8.6
G	28days	52.8	28.1
	About 1year	41.0	11.8

3.2 Expansion

Table 4 shows the expansions of the beam specimens after one year of accelerated ASR deterioration just before the loading test. Figure 7 shows examples of expansion changes with time. In the table, the values in the column “upper longitudinal” show the averages of expansions determined by gauges 1 and 3, the values in the column “lower longitudinal” show the averages of expansions determined by gauges 2 and 4, and the values in the column “vertical” show the averages of expansions determined by gauges 5, 6, 7 and 8. Vertical expansions were larger than longitudinal expansions in most specimens. This is because the beams were less restrained in the vertical direction due to the smaller amount of reinforcement. The upper half along the longitudinal direction showed larger expansions than the lower half, which is due to the tensile reinforcement arranged at the bottom of the beams. As a result, all the beams were visibly arched (Figure 8).

Table 4: Average expansion (and its standard deviation) by ASR after 1 year (unit: micro)

	Lower longitudinal	Upper Longitudinal	Vertical
SG-D6 (4beams)	959 (422)	3456 (575)	4107 (5106)
G-D6 (4beams)	1767 (604)	4348 (912)	5392 (3220)
SG- ϕ 3 (4beams)	1355 (1756)	4645 (1221)	6410 (3913)
G- ϕ 3 (4beams)	729 (602)	3918 (1179)	7288 (3461)
SG-0 (4beams)	1231 (230)	3539 (1023)	7106 (4564)
G-0 (4beams)	1520 (586)	2481 (775)	7433 (2990)

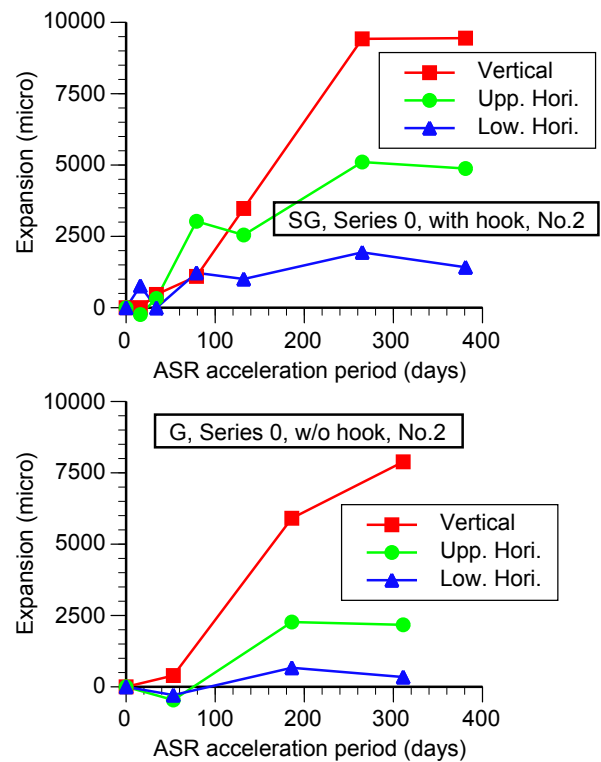


Figure 7: Examples of expansion changes with time

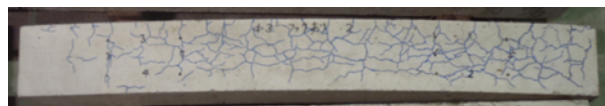


Figure 8: Arched shape of ASR deteriorated beam

While the presence of hooks did not affect the expansions, Series ϕ 3 and Series 0 beams showed generally greater vertical expansions than Series D6 beams which is considered to be because of the difference in the amount of

stirrups, i.e., the degree of restraint. As for the type of mixtures, the specimens with mixture SG showed slightly larger expansions than the specimens with mixture G at early ages. This is attributable to the difference in the specific surface area between fine and coarse aggregates, which resulted in the difference in expansion rate. However, there was no distinct difference in the final expansions between mixtures SG and G at the final stage.

As can be seen from Figure 7, the beams expanded rapidly between 100 and 200 days of age, then the increase slowed down after 200 days. Since all the specimens showed this tendency, the loading test was carried out at the age of one year.

4 MECHANICAL PROPERTIES

4.1 Calculation of beam strength

Table 5 shows the bending and shear capacities of the beams calculated from the compressive strength test results of Table 3. Irrespective of the type of concrete, Series D6 beams have a higher shear capacity than bending capacity, while Series 0 beams have a lower shear capacity than bending capacity. Thus these beams can be considered as the flexural failure type and the shear failure type, respectively. Series $\phi 3$ beams have more or less the same bending capacity and shear

capacity.

Table 5: Calculated capacity of the beams (kN)

	Bending capacity	Shear capacity		
		D6	$\phi 3$	0
NC	86.7	127.8	87.9	64.0
SG	81.2	118.3	78.4	54.5
G	83.9	122.2	82.3	58.4

4.2 Effects of ASR on beam strength

Table 6 shows the results of the loading test. Figure 9 shows examples of the load-deflection curve of the beams. Even though the compressive strength of ASR-deteriorated concrete was lower than NC concrete and the ASR-deteriorated beams had lower calculated shear capacity than those of NC concrete, the shear failure type beams, i.e., Series $\phi 3$ beams and Series 0 beams, of mixtures SG and G generally showed higher shear strength than the NC beams (apart from a few exceptions). Possible causes of the increase in the shear capacity include chemical prestress induced by the expansion of concrete, and the arched shape of the beams that was formed due to uneven rebar arrangement in the expanding concrete. ASR-induced cracks that were already produced at portions where high shear stress was generated are considered to be

Table 6: Results of the loading test

		NC		SG		G	
		Pmax	failure mode	Pmax	failure mode	Pmax	failure mode
D6	with hooks-1	86.3	bending	79.1	bending	81.0	bending
	with hooks-2	85.5	bending	76.0	bending	82.5	bending
	w/o hooks-1	85.9	bending	78.0	bending	82.0	bending
	w/o hooks-2	89.7	bending	73.8	bending	80.9	bending
$\phi 3$	with hooks-1	62.6	shear	79.3	bending	82.9	bending
	with hooks-2	59.6	shear	82.1	bending	82.5	bending #
	w/o hooks-1	73.5	shear*	79.4	shear bond	80.8	bending
	w/o hooks-2	64.4	shear*	79.1	shear	79.8	bending #
0	with hooks-1	59.4	shear*	66.5	shear bond**	44.3	shear bond**
	with hooks-2	52.3	shear*	70.9	shear bond**	63.1	shear bond** #
	w/o hooks-1	55.6	shear*	61.0	shear*	59.4	shear bond
	w/o hooks-2	64.4	shear*	54.0	shear*	81.1	bending #

Note #: repaired by adding shear reinforcement
 *: with a light degree of bond splitting failure
 **: with a failure at the end of the beam

another factor whereby the shear capacity of ASR-deteriorated beams was higher, since these cracks apparently enlarged as the shear strain increased and thereby prevented formation of new cracks that could lead to a sudden shear failure. The test results confirmed that the shear cracks at the failure in the SG and G concrete beams were wider than those in the NC beams, as shown in Figure 10.

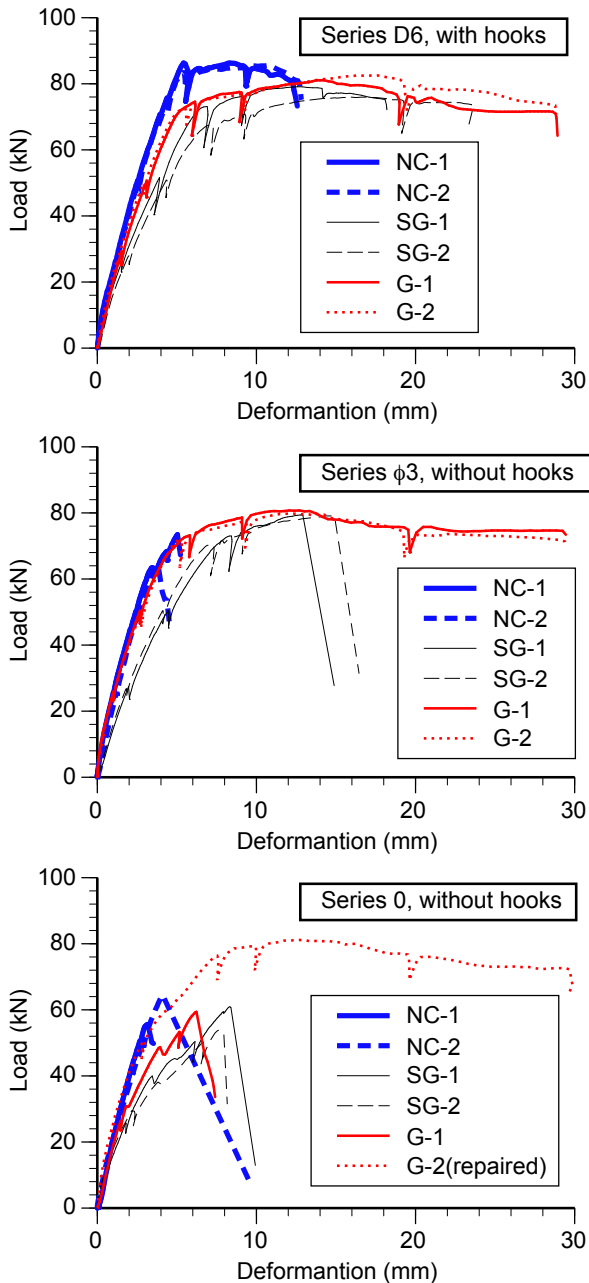


Figure 9: Examples of load-deflection curves

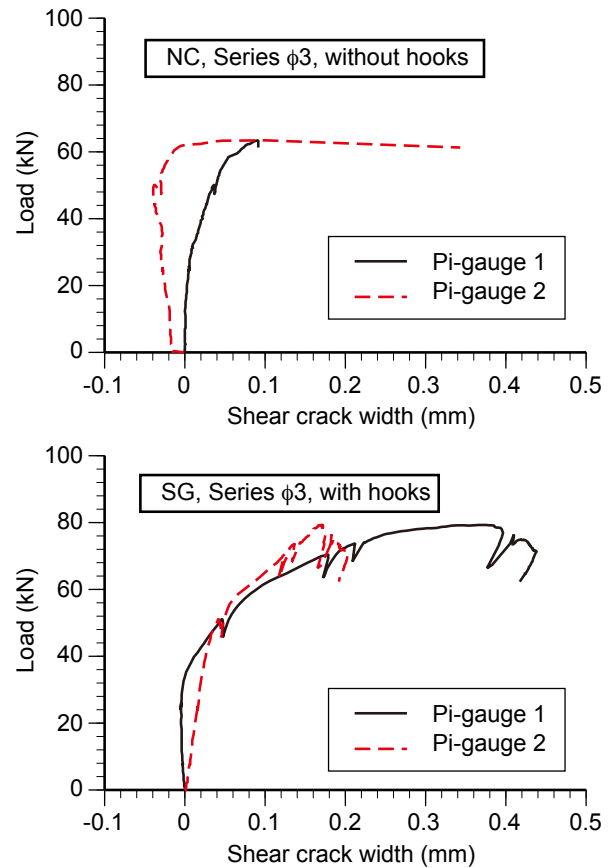


Figure 10: Examples of shear crack propagations

Figure 10 also shows that the SG and G concrete beams have lower stiffness than the NC beams. This is probably because of the significant decrease in elastic modulus of the ASR-deteriorated concrete and also of the presence of the ASR-induced cracks mentioned above.

4.3 Effects of hooks and shear reinforcement

All the specimens of Series D6 reached their failure point when the concrete crushed at the upper surface. There was no apparent difference between the beams with hooks and those without, and therefore the effects of loss of anchorage due to ASR were not observed.

Series $\phi 3$ beams with tensile rebar hooks of mixtures SG and G showed a flexural failure with a concrete crush at the compression surface, while the NC beams showed a shear failure. That is, the failure mode was changed by the effects of ASR-induced deterioration. This change was assumed to be due to the chemical prestress, the presence of ASR-induced cracks, and the formation of the

arched shape, as previously discussed (see Figure 10). Series $\phi 3$ beams without tensile rebar hooks of NC concrete and mixture SG all showed shear failure. One of the SG/Series $\phi 3$ beams without the hooks also showed bond splitting failure at the tensile reinforcement and cover spalling. The tensile rebar without hooks seemed to have lost its bond and anchorage in the cover concrete because of the ASR-induced cracks and concurrent chloride-induced rebar corrosion, resulting in bond-slip of the tensile rebar.

Series 0 beams all exhibited shear failure. The SG and G beams with rebar hooks not only showed the bond splitting failure but also suffered splitting at the beam ends as shown in Figure 11. The failure of concrete around the rebar hooks is attributable also to the loss of the bond and anchorage caused by ASR, which brought about pullout of the tensile rebar. Another factor was the loss of concrete integrity due to the ASR cracks. No clear effects of the type of concrete on the failure mode were observed with Series 0 beams without tensile rebar hooks.



Figure 11: Splitting at the beam ends (SG, Series 0 with hooks)

4.4 Shear repair

The G/Series $\phi 3$ beams that were repaired with additional rebar exhibited bending failure. However, the effects of the shear repair could not be confirmed, because Series $\phi 3$ beams of mixture G that were not repaired, whether with or without rebar hooks, also showed bending failure.

The G/Series 0 beams without rebar hooks that were not repaired showed shear bond failure, while those that were repaired showed bending failure and exhibited much improved strength. The repair with additional rebar is therefore considered to have been effective. On the other hand, while the G/Series 0 beams with rebar hooks that were repaired had higher strength than those that were not repaired, they exhibited shear bond failure as well as the concrete failure around the rebar hooks (see Figure 11) despite the repair.

Figures 12 and 13 show the widths of the shear cracks and the bond cracks in the G/Series 0 beams without rebar hooks, respectively. It is clear from these charts that the repair was effective in suppressing the crack widening at early stages with smaller load. In contrast, such effect of preventing propagation of cracks could not be observed with the beams with hooks. In the repair carried out in this study, the additional rebar was inserted from the upper surface of the beams to as far as the top surface of the tensile reinforcement. Therefore, while the repair with additional rebar is expected to stop further widening of diagonal shear cracks, it cannot prevent propagation of bond-splitting cracks along the tensile reinforcement, especially when the integrity of the concrete has been lost due to ASR-induced cracks. It is considered that the shear failure of the G/Series 0 beams with rebar hooks could not be prevented despite the repair because of the propagation of bond-splitting cracks. Further, the ASR-induced cracks that were already present in the beams when loaded could have affected the failure mode, since the direction of cracks made by the loading depends largely on the size and direction of the cracks that were already there [5]. This is considered to be the reason why the repair was effective only with the beams without the rebar hooks.

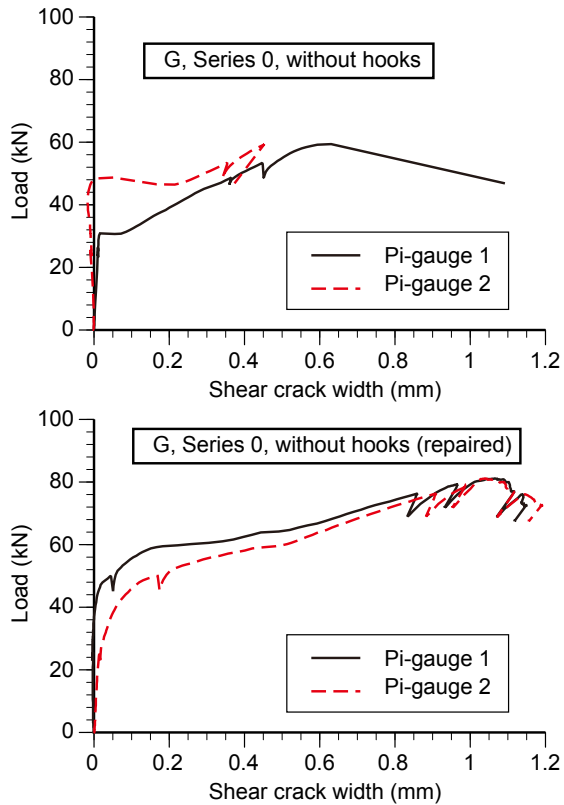


Figure 12 : Effect of shear repair on shear crack propagation

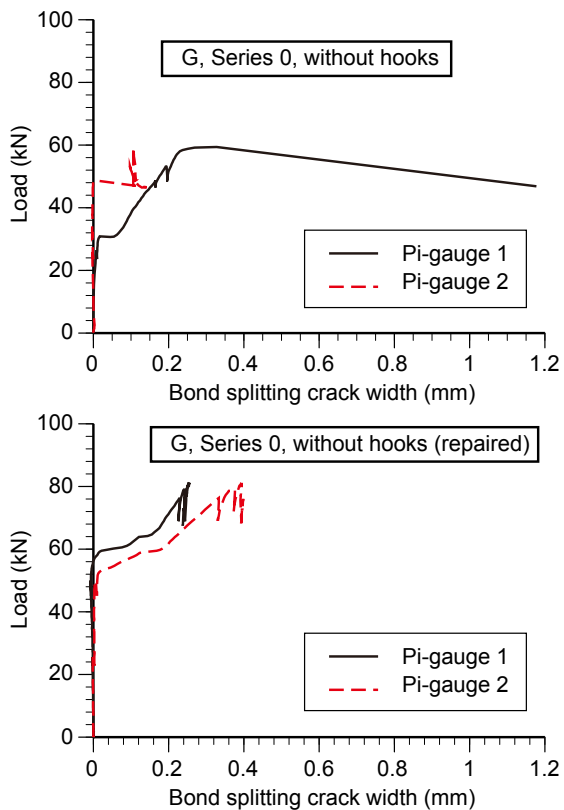


Figure 13 : Effect of shear repair on bond-splitting crack propagation

5 CONCLUSIONS

This study aimed at clarifying the effects of the ASR-induced tensile rebar rapture and shear reinforcement rapture on the mechanical performance of the deteriorated RC members. Model beams were prepared using reactive aggregate and deteriorated in a high-humidity chamber to simulate rapture of the tensile and shear reinforcement, after which they were tested to determine the amount of expansion and mechanical performance. Some of the ASR-deteriorated beams were repaired by adding rebar for the shear reinforcement, and the effects of the repair were investigated.

Results of this study can be summarized as follows;

- Specimens with less amount of shear reinforcement generally showed larger expansion. The expansion rate was faster in the mixture with both fine and coarse reactive aggregates than in the mixture with only coarse reactive aggregate.
- The compression test results confirmed that ASR deterioration caused a significant drop in the elastic modulus of concrete and reduced stiffness of the beams.
- The shear capacity of specimens with less amount of shear reinforcement was increased by ASR.
- ASR-induced cracks reduce the bond/anchorage of the tensile reinforcement. The direction of cracks and the degree of crack propagation may affect the failure mode of deteriorated RC beams.
- The shear repair by adding rebar is not necessarily effective, if the integrity of the concrete has been lost by ASR-induced cracks.

REFERENCES

- [1] Japan Society of Civil Engineers, 2005. *Concrete Library 124, State-of-the-Art Report on the Countermeasures for the Damage due to Alkali-Silica Reaction*. Maruzen. (in Japanese)
- [2] Sawai, K., Takayashi, Y., Osita H., Mikata, Y. and Inoue, S., 2007. *Experimental Study on Shear Resistant*

Mechanism of Reinforced Concrete Beams with Raptured Stirrups Due to ASR. *Proceedings of the Concrete Structure Scenarios, JSMS*. 7:85-90. (in Japanese)

- [3] Hatano, Y., Sawai, K., Mikata, Y. and Inoue, S., 2007. The Fundamental Study on Shear Load Carrying Performance Behaviour of PRC Beam Members with Simulated ASR Expansion. *Proceedings of the Concrete Structure Scenarios, JSMS*. 7:91-96. (in Japanese)

- [4] Hatano, H., Nakashima, T., Harada, Y. and Rokugo, K., 2011. Shear Reinforcement of RC Members using Post-reinforcing bars, *Proceedings of the Japan Concrete Institute*. 33(2):1369-1374. (in Japanese)

- [5] Uchida, Y., Morimoto, H. and Tsukamoto, T., 2001. Post-peak behavior of RC beam with Shear failure, *The 56th JSCE Annual Meeting Proceedings*. V-443. (in Japanese)